

Lawrence Berkeley National Laboratory

LBL Publications

Title

Effects of natural soiling and weathering on cool roof energy savings for dormitory buildings in Chinese cities with hot summers

Permalink

<https://escholarship.org/uc/item/9tt1x923>

Authors

Shi, Dachuan
Zhuang, Chaoqun
Lin, Changqing
et al.

Publication Date

2019-09-01

DOI

10.1016/j.solmat.2019.110016

Peer reviewed

This document is a pre-print of the following publication:

Shi, D., Zhuang, C., Lin, C., Zhao, X., Chen, D., Gao, Y., & Levinson, R. (2019). Effects of natural soiling and weathering on cool roof energy savings for dormitory buildings in Chinese cities with hot summers. *Solar Energy Materials and Solar Cells*, 200(June), 110016. <https://doi.org/10.1016/j.solmat.2019.110016>

The pre-print may lack improvements made during the typesetting process. If you do not have access to the publication, you may request it from Ronnen Levinson at Lawrence Berkeley National Laboratory (RML27@cornell.edu).

1 **Effects of Natural Soiling and Weathering on Cool Roof Energy Savings for Dormitory**
2 **Buildings in Chinese Cities with Hot Summers**

3

4 **Dachuan Shi^a, Chaoqun Zhuang^a, Changqing Lin^a, Xia Zhao^b, Dongping Chen^c, Yafeng Gao^{a*},**
5 **Ronnen Levinson^d**

6

7 ^a Joint International Research Laboratory of Green Building and Built Environment, Ministry of Education,
8 Chongqing University, 400044, Chongqing, PR China

9 ^bXiamen Academy of Building Research Group Co., Ltd., 221116, Xiamen, PR China

10 ^cSichuan Institute of Building Research, 610081, Chengdu, PR China

11 ^dLawrence Berkeley National Laboratory, 1CyclotronRoad, MS90R2000, Berkeley, CA94720, USA

12 * Corresponding author:

13 Email Address: gaoyafeng79@126.com

14 Tel: +86 02365128079

15

16 **Effects of Natural Soiling and Weathering on Cool Roof Energy Savings for Dormitory**
17 **Buildings in Chinese Cities with Hot Summers**

18

19 **ABSTRACT**

20 Roofs with high-reflectance (solar reflectance) coating, commonly known as cool roofs, can stay
21 cool in the sun, thereby reducing building energy consumption and mitigating the urban heat island.
22 However, chemical-physical degradation and biological growth can decrease their solar reflectance
23 and the ability to save energy. In this study, the solar spectral reflectance of 12 different roofing
24 products with an initial albedo of 0.56–0.90 was measured before exposure and once every three
25 months over 32 months. Specimens were exposed on the roofs of dormitory buildings in Xiamen
26 and Chengdu, each major urban areas with hot summers. The albedos of high and medium-lightness
27 coatings stabilized in the ranges 0.45–0.62 and 0.36–0.59 in both cities, respectively. This study
28 yielded albedo loss exceeded those reported in the latest Chinese standard by 0.08-0.15. Finally,
29 DesignBuilder (EnergyPlus) simulations estimate that a new cool roof with albedo 0.78 on a six-story
30 dormitory building will yield annual site energy savings (heating and cooling) for the top floor, which
31 are 8.01 kWh/m² (24.2%) and 9.12 kWh/m² (26.3%) per unit floor area in Xiamen and Chengdu,
32 respectively; while an aged cool roof with albedo 0.45 and 0.56 will yield the annual savings by 5.12
33 kWh/m² (15.4%) and 2.47 kWh/m² (10.5%) in these two cities.

34 **Key Words**

35 High-reflectance coating; Cool roof; Dormitory; Solar reflectance; Energy savings.

36

37 1. Introduction

38 The building sector consumed 40% of global energy and led to considerable carbon emission,
39 consequently it is imperative to improving the energy performance of the building and concurrently
40 ensuring a desirable indoor environment [1]. In China, the energy consumption caused by roof heat
41 transfer accounts for 35% of the total consumption for top floor areas [2]. High-reflectance building
42 roof surfaces with high albedo (solar reflectance), known as “cool roofs”, have been used to prevent
43 overheating of buildings by solar radiation control, reduce the cooling energy need and peak loads
44 of buildings, mitigate heat island effect, and reduce carbon emissions [3][4][5]. Cool roofs have been
45 credited or prescribed in building energy efficiency standards for China [6], especially in hot summer
46 climate areas (hot summer/cold winter and hot summer/warm winter zones).

47 The albedo of high-reflectance coatings has been found to decrease shortly after installation,
48 which is known as natural aging. Many experimental studies have been performed on the impacts
49 of natural aging, and some of them found that the albedo loss had certain characteristics. Dornelles
50 et al. [7] researched the natural aging of 12 roofs with standard paint and 8 roofs with high-
51 reflectance paint in São Paulo, Brazil, and found that the albedo sharply decreased to 0.50 from 0.74
52 within the first 6 months. Additionally, Paolini et al. [8] exposed white and beige finish coats for four
53 years in Milan, and found the solar reflectance of the white finish coats dropped to 0.55 from 0.75 in
54 four years, and to 0.38 from 0.46 for the beige coats, while the thermal emittance was unchanged.
55 Sleiman et al. [9] observed changes to the albedos of hundreds roof products at three sites in the
56 United States after three years outdoor exposure, and found that the albedo of some initially bright-
57 white field-applied coatings (initial value of 0.90) fell to about 0.60 in Phoenix (Arizona), to about
58 0.40 in Cleveland (Ohio), and to about 0.30 in Miami (Florida), respectively.

59 The progressively lowering of their thermal performance and energy savings were convinced
60 being impacted by natural aging [9]. Paolini et al. [10] tested the albedo of 12 roofs (initial albedo
61 above 0.80) of commercial buildings in Roma and Milan, Italy for a period of two years and found
62 that the albedo decreased by 0.14 and 0.22 respectively; and each time the albedo decreased by
63 0.10, the cooling load of buildings increased by 4.1-7.1 MJ/(m²·y). In order to study the cool roof
64 effect at different height of occupants' body, Pisello, A. L et al. [11] compared the indoor thermal
65 comfort conditions generated within the vertical cross section of the attic between the cool and

66 traditional roof configurations in Italy, and they found 2.79 K and 1.54 K air temperature difference
67 in summer and winter, respectively. Mastrapostoli et al. [12] found that the surface temperature of
68 aged cool roofs (albedo 0.50–0.55) was 7–12 K higher than those with new cool roofs (albedo 0.71–
69 0.74), and the school building simulations in Kaisariani, Greece included an application of new cool
70 roof coating, which could decrease the energy demand for cooling by 72%, as compared to the aged
71 cool roof.

72 The changes to solar reflectance result primarily from retention of deposited soiling matter, such
73 as soot, dust, and salt, and biological growth when high reflectance coatings are exposed to
74 environmental conditions (wind, sunlight, rain, hail, snow, and atmospheric pollution) [13][14][15][16].
75 This retention (deposition minus removal) depends on local air quality and local weather (e.g., rain),
76 and is therefore tied to the city. For instance, Aoyama [17] considered black carbon particles as the
77 main component of soil disposition in Japan, while Gao et al. [3] affirmed fog and haze (i.e., PM_{2.5}
78 and O₃) soiled the cool roof surface and caused its albedo loss in Chongqing, China. The natural
79 aging of cool roofs is mainly due to the retention of deposited soiling, such as soot, dust, salt, and
80 biological growth when exposed to the outdoor environment. Since different exposure conditions led
81 to special degradation results; hence, it is necessary to conduct local research on natural aging of
82 cool roofs in China.

83 To maintain maximum cooling energy savings throughout the service lifetime, cool roofs should
84 be cleaned regularly in some cases. Levinson et al. [18] investigated the albedo of 15 single-ply
85 roofing membranes before and after cleaning, and compared the albedo of these after natural aging
86 with those of new membranes; the ratios were 0.41–0.89, those after scrubbing were 0.53–0.95,
87 those after washing were 0.74–0.98, those after cleaning were 0.79–1.00, and those after bleaching
88 were 0.94–1.02. Although cleaning can maintain the albedo of cool-roof, the energy cost savings
89 cannot cover the labor cost [19]. In addition, further research works involve some self-cleaning high
90 reflectance coating, consisting of a photocatalyst system with titanium oxide, or an alkyl silicate
91 system; solar reflectance decreased by 5–10% (to 77–82% from 87%) with self-cleaning coating and
92 by 20–23% (to 64–67% from 87%) with common cool-roof coating in 3–6 months. However, the self-
93 cleaning coating has become somewhat expensive recently [17][20][21].

94 Various evaluation methods, outdoor-exposure trials and laboratory aging practice (ASTM
95 D7897 Standard Practice for Laboratory Soiling and Weathering of Roofing Materials to Simulate
96 Effects of Natural Exposure on Solar Reflectance and Thermal Emittance), for the aging of the cool
97 roof have been studied. Researchers at Lawrence Berkeley National Laboratory (LBNL) have developed
98 a calibrated laboratory aging practice that replicates in less than three days the changes in solar
99 reflectance and thermal emittance that roof surfacing materials experience after three years of
100 natural exposure in various U.S. climates [22][23][24]. Nevertheless, it is challenging to reproduce
101 and match the natural aging of cool-roof coatings in actual soiling (deposition of soot, dust, and salt,
102 and biological growth) and weathering (meteorological conditions) conditions in the laboratory.
103 Therefore, this study will provide the method and engineering case for natural soiling and weathering
104 on high reflectance coatings and standard promotion, especially in Chinese cities with hot summers,
105 where high-reflectance cool roofs are most effective [6]. Meanwhile, natural aging of the high-
106 reflectance coatings can be used to calibrate a laboratory aging practice.

107 Energy Star (ES) and the Cool Roof Rating Council (CRRC) in the US have established perfect
108 product labeling and rating programs for high reflectance coatings [25][26]. To qualify for the
109 ENERGY STAR label issued by the U.S. Environmental Protection Agency's ENERGY STAR
110 program, a low-slope roofing product must demonstrate an albedo of at least 0.65 when new, and
111 an albedo of at least 0.50 three years after installation. The Cool Roof Rating Council (CRRC)
112 establishes a practice for rating the initial and aged solar reflectance and thermal emittance of roofing
113 products [27], and provides a directory of product ratings [25]. However, it does not set performance
114 requirements for cool roofing products [28]. These test methods and product ratings are also
115 recognized by the Green Globes, the Leadership in Energy and Environmental Design (LEED),
116 California Energy Commission (CEC), and ASHRAE [29][30][31][32]. Nevertheless, the latest
117 Chinese standard, *Building Reflective Thermal-insulating Coatings (JG/T 235-2014)*, just stipulates
118 the initial albedo of the following three types of coatings: low lightness (solar reflectance $\rho \leq 0.40$),
119 medium lightness ($0.40 < \rho < 0.80$), and high lightness ($\rho \geq 0.80$), whereas it does not specify the
120 albedo of high reflectance coatings after natural aging.

121 In general, although the cool roofs have been widely used in Chinese cities with hot summers,
122 some problems are not fully addressed including 1) the natural aging characteristics of high-reflective

123 coatings in conditions of specific climate and air quality in China; 2) the impacts of albedo decrease
124 and occupant heating usage habits on energy consumption in dormitory buildings. This study
125 therefore investigates the natural aging characteristics of 12 roofing products, and analyzes the
126 aging effects on energy consumption of the top-floor in a prototype dormitory building in two
127 representative cities (Chengdu and Xiamen), located in hot summer climate regions in China.

128 **2. Natural exposure trials**

129 The following section represents the natural exposure trials in Xiamen and Chengdu by
130 describing the selected materials (Section 2.1), detailing the exposure procedure and climate zone
131 (Section 2.2), and outlining the measurement method (Section 2.3).

132 **2.1 Selected materials**

133 As per *Building Reflective Thermal-insulating Coatings (JG/T 235-2014)*, seven high-reflectance
134 roof coatings of two lightness types (high and medium lightness) are available in the market, with
135 initial solar reflectance (R_i) ranging between 0.56 and 0.90. Two of these roofing products, C6 (WC,
136 high lightness) and C7 (BC, medium lightness), were exposed and measured in Xiamen, and other
137 products (C1-C5) were exposed and measured in Chengdu (Table 1).

138 Twelve roofing products were coated on smoothly polished concrete tiles and aluminum
139 substrates (both with the configuration of 100 mm × 100 mm × 10 mm). These two types of samples
140 (i.e. tiles and substrates) stand for the commonly-used roofs in residential buildings (with a dry-film
141 thickness around 500 μm) and industrial buildings (with a dry-film thickness around 25 μm),
142 respectively. The initial solar reflectance was measured using a Perkin-Elmer Lambda 950 UV-vis-
143 NIR spectrometer, operated in accordance with ASTM E903-12: Standard Test Method for Solar
144 Absorptance, Reflectance, and Transmittance of Materials Using Integrating Spheres [33], and
145 thermal emittance was measured with a portable emissometer emittance, those of selected roofing
146 products were listed in Figure 1. In addition, we included only flat products whose radiative properties
147 could be readily measured using ASTM methods. The selected roofing products comprise with
148 different spectral reflectance and open porosity.

149

150 Table 1. Selected high-reflectance roof coatings for the natural exposure trails in Xiamen and
151 Chengdu.

152

153 Figure 1. Roofing products labeled with initial values of solar reflectance (ρ), thermal emittance (ϵ),
154 lightness color coordinate (L), red/green color coordinate (a), and yellow/blue color coordinate (b).

155 **2.2 Natural (outdoor) exposure procedure, local climate zone, and building prototype**

156 Selected coatings were brushed or sprayed on prototype specimens, which were applied on a
157 concrete tile or aluminum substrate (Figure 2a, b), and they were measured in two experiment sites
158 for comparison purposes. As shown in Figure 2c, d, and Figure 4, the specimens with the same
159 coating were placed on a specimen stand with the configuration of 1,410×1,180mm.

160

161 Figure 2. (a) Concrete tiles, (b) aluminum substrate specimens, (c) side view of the specimen holder;
162 (d) top view of the specimen holder.

163 Since WR can significantly reduce the building energy consumption in hot summer climate zone
164 in China [35], the practical applications of cool roofs have been highly promoted by the government.
165 However, the actual energy savings are determined by the actual performance of the cool coatings
166 (i.e., the aged albedo of the coating). In this study, two representative cities, Xiamen and Chengdu,
167 located in the hot summer regions, are selected to explore the natural aging characteristics of
168 coatings and its effects on building energy consumption. The specimens painted with different
169 coatings were exposed at rooftops in two sites: Xiamen (24.48 °N, 118.08 °E, 23 m height, hot
170 summer and warm winter region) and Chengdu (30.67 °N, 104.07 °E, 19 m height, hot summer and
171 cold winter region), as shown in Figure 3. As highlighted in Section 1, the main causes of roof soiling
172 and albedo loss are from pollution and weathering. The values of several parameters, including wind
173 velocity, air dry-bulb temperature, relative humidity, air quality index and precipitation, are well-
174 recorded in the smart weather station in exposure site (first three parameters) and local weather
175 station (last two parameters).

176

177 Figure 3. Chinese climate zones, Chengdu and Xiamen cities location.

178

179 Each experiment sites were located in a residential area and at a distance from the primary
180 source of pollution (i.e., power plant). One set of specimens was exposed at the low slope (2%,

181 corresponding to a 1.1° tilt), while a duplicate set was exposed at the high slope (20%, corresponding
182 to a 36.4° tilt). Specimens were exposed facing south with 1.5m away from the parapet to prevent
183 being shaded (Figure 5).

184 The solar reflectance of the C1-C5 specimens was measured with an interval of three months
185 from December 2014 to June 2016 in Chengdu (Figure 1). The solar reflectance of these specimens
186 was also measured before exposure (i.e. 0 month) for the purpose of comparison. Similarly, between
187 January 2015 and July 2016, an exposure test was also conducted in Xiamen (Figure 1) to assess
188 the variation of solar reflectance caused by different aging conditions. The two cities are both in hot
189 summer regions. As the test in Xiamen was interrupted due to the typhoon in July 2016, the solar
190 reflectance of C6 and C7 specimens was measured every three months until the 18 months (i.e.
191 June 2016). Although some research works have found the emittance of high reflectance coatings
192 did not decrease after natural aging [9][17], the hemispherical emittance of selected coatings was
193 also measured every three months after exposure. It was ensured that the sampling day and a few
194 days before were not rainy in case of contamination cleaning. One specimen of each category was
195 taken to the laboratory for further measurement every week, while the other specimens were still
196 exposed outdoor. Three different spots on each specimen were selected for solar reflectance
197 measurement while the mean values of the measured solar reflectance were used for analysis. It
198 should be noted that the measured specimens were stored and no longer used for exposure test.

199

200 Figure 4. Natural outdoor-exposure of specimens (a) specimens location, and (b) exposure site.

201 **2.3 Measurement method**

202 This study includes the following steps for each specimen:

- 203 • Measurement of spectral reflectance over the solar spectrum 300–2,500 nm at an interval of
204 5.0 nm.
- 205 • Calculation of solar reflectance.
- 206 • Measurement of the hemispherical thermal emittance.

207 The near normal-hemispherical solar spectral reflectance of prototype specimens (300 nm-2500
208 nm) was measured with a Perkin-Elmer Lambda 950 UV-vis-NIR Spectrometer. The machine was
209 equipped with a 150 mm integrating sphere and operated in accordance with ASTM E903-12:

210 Standard Test Method for Solar Absorptance, Reflectance, and Transmittance of Materials Using
211 Integrating Spheres [33] and JG/T 235-2014: Architectural reflective thermal insulation coating [34].
212 Solar reflectance was calculated by averaging over solar spectral reflectance weighted with solar
213 spectral irradiation.

214 Hemispheric thermal emittance ϵ was measured with a Devices & Services model AE1 portable
215 emissometer, operated in accordance with ASTM C1371-15: Standard Test Method for
216 Determination of Emittance of Materials Near Room Temperature Using Portable Emissometers [35].

217 **3. Case study of dormitory building energy simulation**

218 **3.1 Simulation tool, modelling, and parameters setting**

219 The change to the solar reflectance over time after outdoor exposure provides an indication of
220 the possible variation in the surface heat transfer of the building roof, thereby providing a deeper
221 insight into the impact of albedo changes on the top floor area cooling and heating loads. Previous
222 works [7][8][9] indicate that the service life of a cool roof is expected to last for 20 years, the albedo
223 of cool roof sharply decreases only within the first 6 months and then stabilizes in 2 to 3 years.
224 Therefore, considering the whole service life of cool roofs, it is reasonable to simulate the energy
225 savings neglecting the changes of solar reflectance at the first 2 to 3 years.

226 In this study, a representative six-story dormitory building model was constructed in
227 DesignBuilder v5.3. Designbuilder was selected as the tool for the case study as it is relatively
228 accurate for energy simulation [36][37]. Crawley et al. [38] consider it as a mature product which
229 offers flexible geometry input and extensive material libraries and load profiles. EnergyPlus is
230 integrated within Designbuilder's environment which allows it to carry out complete simulations
231 without leaving the interface. Designbuilder has quality control procedures which assure the
232 accuracy of the results in comparison with the standalone EnergyPlus engine [39].

233 The building model was based on prototype of a concrete-slab (foundation, walls, and roof)
234 dormitory building in Xiamen, which was modelled measuring 626.3 m² conditioned floor area and
235 north-south oriented with windows on the south and north facades. The envelope characteristics,
236 ventilation and infiltration rates, internal loads, operating schedules, and cooling and heating set
237 points to comply with the prescriptive requirements or recommended design values in current
238 Chinese building energy efficiency standards (see parameters in Table 3, Table 4, and Figure 5)

239 [41], and were made to reflect the typical details in hot summer climates, as shown in Table 2 and
240 Table 3. The exterior climate data were defined by hourly typical meteorological year (TMY) from the
241 Chinese Standard Weather Data (CSWD) [42].

242

243 Figure 5 (a) Axonometric rendering projection and (b) plan of the top floor of the representative
244 dormitory building simulated.

245

246 Table 2. Characteristics of the top floor of the representative office building simulated.

247

248 Table 3. Roof and wall construction (listed outside to inside) of a representative dormitory building
249 in each city [34].

250 The HVAC system was designed based on the Chinese building energy efficiency standards
251 and detailed in Table 2. The setpoint temperature was 26 °C in summer and 16 °C in winter. Space
252 cooling and heating were provided by split direct expansion air-source heat pumps, which are
253 commonly used in China [6]. The cooling and heating COPs of the air conditioning system are 3.0
254 and 2.5, respectively. In the simulation, the indoor air temperature was set to maintain the room in
255 a comfortable temperature range (cooling setpoint of 26°C; heating setpoint of 16°C, Table 2), and
256 indoor temperature and humidity were assumed evenly distributed.

257 **3.2 Case study**

258 In order to estimate the impact of natural aging of high-reflectance coatings on the energy
259 savings of cool roofs in Chinese cities with hot summer climates, six case studies were considered
260 in this paper: the building model with a grey roof (with an aged albedo of 0.20) was simulated in
261 Chengdu and Xiamen and used as the reference buildings. The building models with an aged cool
262 roof and a new cool roof in Xiamen and Chengdu, respectively. In addition, the case in Xiamen
263 comprised two scenarios, including space heating and no space heating, because Xiamen is
264 located in hot summer/warm winter zone and does not take into account heating. Zhuang
265 investigated the air conditioning service in Xiamen and found about 40 % of households use air-
266 conditioned heating in winter [40]. In these cases, the albedo before and after aging was selected
267 according to measured data, the building with a new high-reflectance coating was modelled as

268 0.68 and 0.80 in Xiamen and Chengdu (median values of new high-reflectance coatings in two
269 cities), respectively, and the values of aged cool roof simulation corresponded with the median
270 values of outdoor exposure measurement data after 30 month in Xiamen and Chengdu.

271 Space heating load and space cooling load savings were computed as the load of the building
272 with the reference (grey) roof minus that of the building retrofitted with the aged cool roof. The site
273 cooling/heating energy savings can be estimated by dividing the cooling/heating load savings with
274 the corresponding COPs, respectively.

275 **4. Natural exposure trials results and discussion**

276 **4.1. Natural exposure trials**

277

278 Figure 6. The solar reflectance of selected roofing products (aged - initial solar reflectance), (a)-(e)
279 shows the ten specimens exposed in Chengdu, while (f) shows the two specimens exposed in
280 Xiamen.

281 The initial albedo ρ_i of each high-lightness coating (C1, C3, or C5; $\rho_i \geq 0.80$) applied to a
282 concrete substrate was about 0.02 higher than that of the same coating applied to an aluminum
283 substrate (Figure 6 a-e), while medium-lightness coatings ($\rho_i < 0.80$) yielded the same initial
284 albedos over concrete and aluminum.

285 Figure 6 shows the evolution of albedo over the 30-month natural exposure trials conducted in
286 Chengdu from January 2015 to June 2017 (Figure 6 a-e), and over the 18-month test performed in
287 Xiamen from December 2014 to June 2016 (Figure 6f). In Chengdu, the albedos of selected
288 specimens (C1-C5) decreased by 0.20 between months 0 and 3 (January 2015 to April 2015), and
289 another wide range of albedo losses by 0.03-0.16 occurred in the heating season (i.e., November
290 2016 to February 2017). Paolini found similar results for roofing and walling membranes in Roma
291 and Milano [9][7] as the heating season yielded the main value loss during the exposure (Figure 6).
292 After one year of exposure, no remarkable albedo loss was measured in C3 and C4, while the
293 albedos of C1 and C2 increased by 0.05 between months 3 and 9. The albedos of C1, C2, and C5
294 did not decrease monotonically, and they increased sharply by 0.07-0.12 between months 15 and
295 18 and between months 24 and 31, corresponding to the rainy seasons (March through July) in
296 years 2016 and 2017 (Figure 7). After 30 months of natural aging, the mean albedo loss of the C1,

297 C2, and C5 specimens was 0.23. Meanwhile, the albedos of C3 and C4 remained stable until the
298 end, as no remarkable loss or increase in heating seasons or rainy season between months 15 and
299 24, and the value loss of C3 and C4 measured between 0.36–0.41 and 0.36–0.37 in month 30,
300 respectively.

301 For the high-lightness coatings in Xiamen, C6 with albedo greater than 0.56 remarkably lost
302 0.23 between months 0 and 10 (i.e., December 2014 to September 2015), which yielded 74.2% of
303 the total value lost. Meanwhile, the most substantial decrease of 0.13 occurring between months 0
304 and 3 during the first heating season (i.e., December 2014 to February 2015), and there was no
305 albedo decrease of the same magnitude in the next winter. Between months 11 and 18 (i.e., Oct
306 2015 to Jun 2016), significant reductions were not measured. During the initial drop period between
307 months 0 and 10, the pace of albedo decrease of C6 slowed gradually, and stability was achieved
308 for most of the exposed products.

309

310 Figure 7. Daily mean wind velocity, monthly mean air temperature, relative humidity and average
311 precipitation in Chengdu and Xiamen.

312

313 Different trends of coating albedo between these two cities are due to 1) Xiamen is warmer
314 (average 16.5°C) than Chengdu (average 9°C) during winter; 2) average wind speed in Xiamen was
315 higher than that in Chengdu (3.0 m/s versus 0.9 m/s as shown in Figure 7). Therefore, more building
316 heating and dust deposition and weaker cleaning mechanism (low wind speed and less rainfall)
317 resulted in severer air pollution concentration in Chengdu, especially in winter. Accordingly, Figure
318 8 shows the severe air pollution occurring between months 11 and 14 (114.7-172.3 $\mu\text{g PM}_{2.5}/\text{m}^3$),
319 and between months 22 and 26 (89.6-123.5 $\mu\text{g PM}_{2.5}/\text{m}^3$) in Chengdu, corresponding to the sharp
320 albedo losses in panels a, b, and e of Figure 6.

321

322 Figure 8. The monthly average Air Quality Index (AQI) in Chengdu and Xiamen (Dec 2014 or Jan
323 2015). AQI presents the daily mean concentration of areal PM 2.5. Higher daily mean concentration
324 indicates higher the index level (i.e., I is excellent; II is good; III is light pollution; IV is moderate

325 pollution)[41]. AQI data were provided by local weather stations with short distance to the exposure
326 site.

327

328 Additionally, different albedo changes were caused by differences between the air quality and
329 rainy conditions in two cities. For C1-C5 in Chengdu, with distinct dry and rainy seasons (Figure 7),
330 the loss of the albedo was even due to the retention of dust and airborne particulate (e.g., between
331 month 3 and 9). While in the rainy seasons (e.g., between month 15 and 18, or after month 24),
332 when air quality was good, the albedos increased due to rain wash. However, for C6-C7 in Xiamen
333 with much more annual rainfall and high relative humidity (Figure 7), due to the high air quality, the
334 albedo of coatings was decreased slowly in Xiamen (Figure. 6f).

335 Medium-lightness coating C7 had the lowest initial albedo (0.56). After 18 months, its albedo
336 fell by 0.19 (33%). The albedo variation of C7 stabilized earlier than that of C6; C7 lost 0.12 in albedo
337 between months 0 and 7 (i.e., initial to May 2015), which yields 63.5% of its total value lost. In the
338 following 8 months (i.e., May 2015 to January 2016), the albedo showed a downward fluctuation
339 over time, sometimes exceeding the albedo measured in the earlier three months between months
340 11 and 13 (i.e., measured 0.43 in Feb 2016). Due to the decrease of precipitation intensity in these
341 months (Figure 4), soot deposits on the specimens resulted in albedos fluctuations. Similar
342 fluctuations were also shown in low-reflectivity membranes ($\rho=0.20-0.30$) and glossy single-ply
343 membranes in some cases [9][42]. Different from C6 with 2.0% slope, the most substantial
344 decreases occurring during the rainy season (i.e., February to June in 2015, Figure 7), albedo of the
345 C7 dropped by approximately 0.02, and in the next rainy season (i.e., February to June in 2016,
346 Figure 7), the precipitation intensity increased again, thereby cleaning the deposited soot resulting
347 from the substantial decreases.

348 The coatings exposed and tilted by 20% (pitched roof) in Xiamen and Chengdu showed similar
349 tendency as the same coatings at 2% slope (Figure 6a-f). All selected coatings finished on concrete
350 tile and aluminum substrate showed root mean deviation of less than 0.034 (average of 0.024) and
351 0.023 (average of 0.018) after 30 months of exposure respectively. In addition, the selected coatings
352 finished with a field-applied coating on concrete tile and factory-applied coating on aluminum
353 substrate exhibited similar trends, excluding C3 in Figure 6c (i.e., March to December 2016). All

354 other selected coatings finished on concrete tile compared to aluminum substrate showed root mean
355 deviation of less than 0.024 (average of 0.020) after 30 months exposure in Chengdu. Therefore,
356 the intensity of the effects does not seem to be highly influenced by slope and substrate in the four
357 categories of selected coatings, except C3.

358

359 Figure 9. Spectral reflectance within ranged 300nm–2500nm after every 3 months with 2%-sloped
360 exposure for coating(a) C6 (high lightness, cement-based) and (b) C7 (medium lightness, cement-
361 based) in Xiamen, (c) C3 (high lightness, cement-based),(d) C4 (medium lightness, cement-based),
362 (e) C7 (high lightness, aluminum-based), and (f) C8 (medium lightness, aluminum-based) in
363 Chengdu.

364 Focusing on the spectral reflectance variation after outdoor exposure (Figure 9), C6 and C3 (for
365 the high-lightness coatings with similar spectra), and C4 and C7 (for the medium-lightness coatings
366 with similar spectra), were exposed outdoors in Xiamen and Chengdu. Spectral reflectance changes
367 were smallest in the UV spectrum (300 – 400 nm) and at the tail end of the NIR spectrum (2,200 –
368 2,500 nm), which had little significance for the surface energy balance [9]. The obvious variation of
369 aged spectra is evident mainly in the VIS and the first portion of NIR (420nm to 2200nm), similar to
370 what was observed by Paolini et al.[7][9]. The inflection points in the aged spectra ranged 420–600
371 nm is compatible with the early physical degradation of the binder of the finish coat due to UV
372 irradiation, weathering, and soot [9], blue wavelength irradiation are also determined (Figure 9) [43].
373 Furthermore, the shape of aged spectra, ranging between 420 nm and 600 nm, is altered as a result
374 of physical degradation. The reflectance of aged spectra between 420 nm and 825 nm attenuated
375 faster so that the shape nearby 825 nm altered after one year; an obvious leap (near 0.02) occurred
376 in all coatings exposed in Xiamen and Chengdu.

377 Additionally, C1 and C2 showed the appearance of cracks after exposure (Figure 10a), which
378 could result from either substrate contraction in winter and expansion in summer, or strong UV
379 irradiation which breaks the chains of macromolecules to create free radicals and form molecular
380 chains, thereby results in chemical-structure changes in their binder, resins, and generate internal
381 stress [44]. After all, it was suggested by pulverization, blistering, cracks noticed after a few months
382 of outdoor exposure, reflectance reduction, shape alteration, and leap in this spectra portion were

383 symptoms of this degradation. There is visual evidence of significant physical disintegration after
384 one year of exposure (Figure 10).

385

386 Figure 10. A feature of aged specimens in months 12 (a) cracks (b) blistering (c) mildew growth.

387 For field-applied C3 (high lightness) and C4 (medium lightness) exposed in Chengdu (Figure
388 9c, e), the shape changed considerably, especially between 420 nm and 600 nm wherein the
389 portions and intensity of the impacts and effects on C3 and C4 in Chengdu are higher than C6 and
390 C7 in Xiamen (Figure 9a, b). The reflectance fell in extreme fashion with the impact of acid rain in
391 Chengdu, as it contained a lot of contaminants, including humic acid and dust surrogates those were
392 determined to drive the albedo loss in the visible and ultraviolet regions [45][46].

393 The spectrum of C7 was almost unchanged between 400 nm and 500 nm (Figure 9b), while for
394 C4, which had higher reflectance (400–750 nm), the average relative loss was higher. The same
395 reflectance recovery is suggested by slight spectra enhancement (i.e., January to July 2016, Figure
396 9c, d), recovery was produced by more rain-wash (Figure 4), and the carbonation and efflorescence
397 of cement-based specimens are transient in effect and highly soluble [46]; therefore, the trend of
398 albedo, in fact, fluctuated for some time.

399 The increase over time of the 1,300–2,300 nm reflectance of C7 in Xiamen may have resulted
400 from the carbonation of concrete tile (i.e., March 2015); the phenomena observed is actually
401 compatible with a residual of calcium carbonate [7]. However, this increase occurred only in the case
402 of C7; therefore, it is not certain that the increase in solar reflectance is prevalent. In addition, C7
403 suffered the least absolute loss (near 0.20), because the absorption coefficient of soot decreases
404 with wavelength [47][48].

405 **4.2. Discussion**

406 After 6 to 12 months of exposure, albedo of high-reflectance coatings decreased rapidly, with
407 albedo losses of 0.25–0.41 and 0.14–0.27 in Chengdu and Xiamen, respectively. The loss in
408 Chengdu was severer than that measured in Chongqing (29.18°N, 106.16°E, close to Chengdu),
409 where an exposure trials of high-reflectance coatings ($\rho_i=0.82$) on an office building were conducted
410 from July 2014 to July 2015 and the albedo decreased 0.20 after one year of exposure [42].

411 Thereafter, the albedo of C1, C2, and C5 fluctuated sharply, and albedo of high-lightness coatings
412 stabilized approximately four months earlier than that of medium-lightness coatings. Considering the
413 severer air pollution in the selected cities in China (shown in Figure 8), After 30 months of exposure,
414 the albedo of high and medium-lightness coatings stabilized in the range between 0.45–0.62 and
415 0.36–0.59, respectively, and the aged values were smaller than the values (near 0.60) measured
416 by Sleiman et al. [49][50]. Additionally, the measured albedo would stabilize in 2 years, which is
417 shorter than the results in the USA. As is shown in Table 4, the latest Chinese standard addresses
418 the albedo loss of high and medium lightness coatings by 0.20 and 0.15, respectively, but the actual
419 albedo loss of C1-C7 exposed in Xiamen and Chengdu exceeded the values addressed by 0.08-
420 0.15, which indicates the standard data according to lab practice is not consistent with exposure
421 trails.

422

423 Table 4. High-reflectance roof standards in China.

424 Although the main causes of natural aging of high-reflectance coatings are almost the same
425 (i.e., deposition of carbon emitted by vehicles or particles from heating furnaces), the trend of albedo
426 value changes was different in Xiamen and Chengdu. This is due to the intensity of the deposition,
427 physical and chemical degradation and biological growth are different in the two cities, as they are
428 affected by local weather conditions (i.e., solar irradiation, precipitation, and air circulation) and air
429 quality. However, the emittance values fluctuated with small changes and maintained stability after
430 exposure in both cities.

431 **5. The impact of aging on the energy performance of the buildings**

432 In order to estimate the impact of the natural aging of high-reflectance coatings on the cooling
433 and heating site energy consumption of dormitory buildings in the hot summer climate of China. The
434 annual simulations of reference buildings with an aged grey roof (albedo of 0.20), new cool roof, and
435 aged cool roof were performed in Xiamen and Chengdu. The boundary conditions used are
436 presented in Tables 2 and 3 (Section 3). In some energy consumption simulation research works,
437 the cool roof simulation used consisted of an aged albedo of 0.60 [51], but the albedo of aged high-
438 reflectance coatings was below this value in the hot climate of China (Section 4.1). Therefore, as the

439 solar reflectance of the aged cool roof stabilized after 2 years in both Chengdu and Xiamen, the
440 albedo of aged cool roof simulation corresponded with the median values of outdoor exposure
441 measurement results in Xiamen and Chengdu, respectively, and the values are shown in Table 5.

442

443 Table 5. Solar reflectance and median values of selected roofing products after outdoor exposure in
444 Xiamen and Chengdu.

445 The previous simulation results indicate that the energy savings scale of the cool roof scale
446 linearly with the change in roof albedo [4]. Figure 11 and 12 depict the annual cooling and heating
447 loads and energy consumptions for the dormitory buildings in Xiamen and Chengdu.

448

449 Figure 11. Annual heating and cooling loads and site energy consumption for dormitory building in
450 Xiamen with scenarios of the new or aged grey roof (albedo 0.20), aged cool roof (albedo 0.45), and
451 new cool roof (albedo 0.78).

452 For the dormitory building in Xiamen, raising the roof albedo to 0.78 (for a new cool roof) from
453 0.20 (for an aged grey roof) decreases the annual cooling load by 24.56 kWh/m², and annual cooling
454 site energy use by 8.18 kWh/m², respectively. It also increases the annual heating load by
455 0.51kWh/m² and annual heating site energy use by 0.17 kWh/m², respectively. The new cool roof
456 can reduce energy consumption for the top floor areas by 24.2% (8.01 kWh/m²). However, a mean
457 albedo loss of 0.33 caused by natural aging increases the specific annual cooling needs by 5.22
458 kWh/m², and it decreases the heating penalty by 0.10 kWh/m², respectively, which is 10.5% energy
459 savings of initial energy savings. Zhuang [40] measured the cooling energy use of an existing
460 dormitory building retrofitted with an aged cool roof (albedo of 0.44) in 2014, and found the energy
461 savings ranged between 4.42–11.44 kWh/m²; it was determined that high-reflectance coatings had
462 more energy savings potential in existing buildings. Additionally, when excluding space heating in
463 winter (the second scenario in Section 3), the winter heating penalty of cool roof does not exist, the
464 aged cool roof can reduce 9.0% energy consumption (2.92 kWh/m²) in the end.

465

466 Figure 12. Annual heating and cooling loads and site energy consumption for dormitory building in
467 Chengdu with scenarios of the grey roof (0.20), aged cool roof (0.56), and new cool roof (0.83).

468 For the dormitory building in Chengdu, annual heating and cooling loads and site energy
469 consumption of the building model applied with a grey roof (0.20), aged cool roof (0.56), and new
470 cool roof (0.83) were simulated (Figure 12). For a new cool roof, the results of the annual energy
471 consumption presented a decrease of 9.12 kWh/m² (26.3%), while a decrease of 6.65 kWh/m²
472 (15.8%) was recorded for an aged cool roof. The simulation results indicated that natural aging
473 reduced the energy savings of high-reflectance coatings by 2.47 kWh/m² (10.5%). Natural aging can
474 reduce the annual heating penalty of 1.37 kWh/m² (35.0%), although the energy savings for cooling
475 with aged cool roof lost 8.64 kWh/m² (20.1%).

476 We computed, instead, a small reduction in the heating penalty after natural aging in both
477 Xiamen (0.10 kWh/m²) and Chengdu (0.46 kWh/m²). The variations we computed are relatively small,
478 but they contribute to increasing the uncertainty in building energy simulation. Thus, aged values for
479 the solar reflectance of walls shall be considered.

480 **6. Summary**

481 This paper conducted an outdoor exposure experiment of 12 available high-reflectance coatings
482 classified by high/medium lightness, flat/pitched roof, and field/factory-applied, with initial solar
483 reflectance between 0.56 and 0.90. Each specimen was exposed on the natural rooftop racks in
484 Xiamen and Chengdu, large Chinese cities with hot summers. During exposure, no obvious
485 differences were noticed between the coatings substrates exposed or specimens tilted by high or
486 low slopes in both Xiamen and Chengdu; after 30 months, the albedos (solar reflectance) of high
487 and medium-lightness coatings stabilized in the range between 0.45–0.62 and 0.36–0.59
488 respectively. The albedos of C1, C2, and C5 fluctuated sharply, and the albedos of high-lightness
489 coatings tended to stabilize four months earlier than those of medium-lightness coatings. The shapes
490 of the spectral reflectance of exposed coatings varied by city. The shapes of the reflectance spectra
491 of the factory-applied coatings differed from those of field-applied coatings before exposure. In
492 addition, the exposure results in Xiamen and Chengdu after exposure trials exceeded the values
493 addressed the latest Chinese standard by 0.08-0.15; this indicates the lab aging data is not
494 consistent with the natural aging measurement.

495 The natural aging of high-reflectance coatings affects the energy savings of dormitory buildings
496 subject to the hot summer climate of China; the representative dormitory building models with grey

497 roof, aged cool roof, and new cool roof were built to simulate the annual heating and cooling loads
498 and site energy consumption in Xiamen and Chengdu. Consider the heating penalty and cooling
499 energy savings, it is shown that the application of new heat reflective roof coating can decrease the
500 annual site energy use for the top floor areas by 8.01 kWh/m² (24.2%) in Xiamen and 9.12 kWh/m²
501 (26.3%) in Chengdu. Albedo decreases following aging reduced these savings to 5.12 kWh/m²
502 (15.4%) in Xiamen and 2.47 kWh/m² (10.5%) in Chengdu, respectively.

503 In this study, the energy consumption simulation was used to reflect the effects of albedo
504 reduction on the energy savings of cool roof. The building prototype model was set based on a
505 prototype of a concrete-slab (foundation, walls, and roof) dormitory building in Xiamen. The
506 parameters, including envelope characteristics, ventilation and infiltration rates, internal loads,
507 operating schedules, and cooling and heating setpoints, comply with the prescriptive requirements
508 or recommended design values in current Chinese building energy efficiency standards. Therefore,
509 the prototype can represent the current dormitory buildings in China. It is also worth noting that the
510 validation is not fully explored in this paper, and the parametrical analysis is needed to be further
511 investigated, to evaluate the energy savings under different building insulation (i.e., high or no
512 thermal insulation).

513 **Acknowledgments**

514 This research work was supported by the National Natural Science Foundation of China (No.
515 51878088).

516 **Reference**

- 517 [1] Joudi, A., Svedung, H., Cehlin, M., & Rönnelid, M. (2013). Reflective coatings for interior and exterior
518 of buildings and improving thermal performance. *Applied Energy*, 103(2), 562-570.
- 519 [2] Wang, L. (2004). *Teaching material for the “Tenth Five-year Plan” for civil higher disciplines in general
520 higher education, recommended teaching materials for the architectural professional guidance committee
521 of universities, and building energy conservation*. China Architecture & Building Press.
- 522 [3] Gao, Y., Shi, D., Levinson, R., Guo, R., Lin, C., Ge J. (2017). Thermal performance and energy savings
523 of white and sedum-tray garden roof: a case study in a Chongqing office building. *Energy & Buildings*,
524 156, 343-359.
- 525 [4] Lei, J., Kumarasamy, K., Zingre, K. T., Yang, J., Wan, M. P., & Yang, E. H. (2017). Cool colored coating
526 and phase change materials as complementary cooling strategies for building cooling load reduction in
527 tropics. *Applied Energy*, 190, 57-63.
- 528 [5] Pisello, A. L., & Cotana, F.. (2015). Thermal-energy and environmental impact of cool clay tiles for
529 residential buildings in Italy. *Procedia Engineering*, 118, 530-537.
- 530 [6] Gao, Y., Xu, J., Yang, S., Tang, X., Zhou, Q., Ge J. (2014). Cool roofs in China: policy review, building
531 simulations, and proof-of-concept experiments. *Energy Policy*, 74, 190–214.
- 532 [7] Dornelles, K., Caram, R., Sichieri, E. (2015). Natural Weathering of Cool Coatings and its Effect on Solar
533 Reflectance of Roof Surfaces. *Energy Procedia*, 78, 1587–1592.
- 534 [8] Paolini, R., Zani, A., Poli, T., Antretter, F., Zinzi, M. (2017). Natural aging of cool walls: impact on solar
535 reflectance, sensitivity to thermal shocks and building energy needs. *Energy & Buildings*, 153, 287–296.
- 536 [9] Sleiman M, Ban-Weiss G, Gilbert HE, Francois D, Berdahl P, Kirchstetter TW, Destailats H, Levinson R.
537 (2011). Soiling of building envelope surfaces and its effect on solar reflectance-Part I: Analysis of roofing
538 product databases. *Solar Energy Materials & Solar Cells* 95, 3385-3399.
539 (<https://doi.org/10.1016/j.solmat.2013.11.028>)
- 540 [10] Paolini, R., Zinzi, M., Poli, T. (2014). Effect of aging on the solar spectral reflectance of roofing
541 membranes: Natural exposure in Roma and Milano and the impact on the energy needs of commercial
542 buildings. *Energy & Buildings*, 84, 333–343.
- 543 [11] Pisello, A. L. , Castaldo, V. L. , Fabiani, C. , & Cotana, F. . (2016). Investigation on the effect of
544 innovative cool tiles on local indoor thermal conditions: finite element modeling and continuous

- 545 monitoring. *Building and Environment*, 97, 55-68.
- 546 [12] Mastrapostoli, E., Santamouris, M., Kolokotsa, D., Vassilis, P., Venieri, D., Gompakis, K. (2016). On the
547 aging of cool roofs: a measure of optical degradation, chemical and biological analysis and assessment of
548 the energy impact. *Energy & Buildings*, 114(3), 191-199.
- 549 [13] Synnefa, A., Santamouris, M., Apostolakis, K. (2007). On the development, optical properties and thermal
550 performance of cool colored coatings for the urban environment. *Solar Energy*, 81(4), 488–497.
- 551 [14] Paroli, R. M., Dutt, O. S., Delgado, A. H. (1993). Ranking PVC Roofing Membranes Using Thermal
552 Analysis. *Journal of Materials in Civil Engineering*, 5(1), 83–95.
- 553 [15] Eilert, P. (2000). High albedo (cool) roofs: Codes and standards enhancement (CASE) study. Pacific Gas
554 and Electric Company,
- 555 [16] Berdahl, P., Akbari, H., & Rose, L. S. (2002). Aging of reflective roofs: soot deposition. *Applied Optics*,
556 41(12), 2355–2360.
- 557 [17] Aoyama, T., Sonoda, T., Nakanishi, Y., Tanabe, J., & Takebayashi, H. (2017). Study on the aging of solar
558 reflectance of the self-cleaning high reflectance coating. *Energy & Buildings*, 157, 92-100.
- 559 [18] Levinson, R., Berdahl, P, Berhe, A. A. (2005). Effects of soiling and cleaning on the reflectance and solar
560 heat gain of a light-colored roofing membrane. *Atmospheric Environment*, 39(40), 7807–7824.
- 561 [19] Bretz, S. E. & Akbari, H. (1997) Long-term performance of high-albedo roof coatings. *Energy &*
562 *Buildings*, 25(2), 159–167.
- 563 [20] H, Akbari. (2014). Advance in developing standards for accelerated aging of cool roofing materials. In
564 *2014 International Roof Coatings Conference*. Washington DC: Roof Coatings Manufacturers
565 Association.
- 566 [21] Fukaumi, H., Hamamura T., Sonoda T. (2015). Coating composition and a coating film obtained from the
567 coating composition. EP2821450A1. European Patent Application,
- 568 [22] Sleiman, M., Kirchstetter, T. W, Berdahl, P. (2014). Soiling of building envelope surfaces and its effect
569 on solar reflectance-Part II: Development of an accelerated aging method for roofing materials. *Solar*
570 *Energy Materials & Solar Cells*, 122(3), 271–281.
- 571 [23] Sleiman, M., Chen, S, Gilbert, H. E. (2015). Soiling of building envelope surfaces and its effect on solar
572 reflectance-Part III: Interlaboratory study of an accelerated aging method for roofing materials. *Solar*
573 *Energy Materials & Solar Cells*, 143, 581–590.

- 574 [24] ASTM. 2018. ASTM D7897-18 Standard Practice for Laboratory Soiling and Weathering of Roofing
575 Materials to Simulate Effects of Natural Exposure on Solar Reflectance and Thermal Emittance. ASTM
576 International, West Conshohocken, PA, 2018. <https://doi.org/10.1520/D7897-18>
- 577 [25] Poli Environmental Protection Agency (EPA). *Energy Star products – roof products*. Retrieved from
578 (HTTP://www.energystar.gov/index.cfm?fuseaction=find_a_product).
- 579 [26] Cool Roof Rating Council (CCRC) *Rated products directory*. Available from
580 (<http://coolroofs.org/products/search.php>).
- 581 [27] CRRC. 2016. ANSI/CRRC S100 (2016): Standard Test Methods for Determining Radiative Properties of
582 Materials. Cool Roof Rating Council, Portland, Oregon. ([http://coolroofs.org/product-rating/ansi-crrc-](http://coolroofs.org/product-rating/ansi-crrc-s100)
583 [s100](http://coolroofs.org/product-rating/ansi-crrc-s100)).
- 584 [28] CRRC. (2018). Overview: About the Product Rating Program. Cool Roof Rating Council, Portland,
585 Oregon. (<http://coolroofs.org/product-rating/overview>).
- 586 [29] LEED-NC. (2005). *The green building rating system for new construction & major renovations*, Version
587 2.2. Washington, DC: US Green Building Council.
- 588 [30] ASHRAE Standard 90.1-2007. (2007). *Energy standard for buildings except for low-rise residential*
589 *buildings*. Atlanta, GA: American Society of Heating, Refrigerating and Air-Conditioning Engineers.
- 590 [31] ASHRAE Standard 90.2-2007. (2007). *Energy-Efficient Design of Low-Rise Residential Buildings*.
591 Atlanta, GA: American Society of Heating, Refrigerating and Air-Conditioning Engineers.
- 592 [32] CEC. 2015. 2016 *Building Energy Efficiency Standards for Residential and Nonresidential Buildings*.
593 *CEC-400-2015-037-CMF*, California Energy Commission, Sacramento, California.
594 (<http://www.energy.ca.gov/2015publications/CEC-400-2015-037/CEC-400-2015-037-CMF.pdf>).
- 595 [33] ASTM. 2012. ASTM E903-12 Standard Test Method for Solar Absorptance, Reflectance, and
596 Transmittance of Materials Using Integrating Spheres. ASTM International, West Conshohocken, PA.
597 <https://doi.org/10.1520/E0903-12>
- 598 [34] Ministry of housing and urban-rural construction. (2014). *Building reflection and heat insulation paint*.
599 The People's Republic of China.
- 600 [35] ASTM C1371-15. (2015). *Standard Test Method for Determination of Emittance of Materials Near Room*
601 *Temperature Using Portable Emisometers*. West Conshohocken, PA: ASTM International.
- 602 [36] Boafu, F. E., Ahn, J. G., Kim, J. T., & Kim, J. H. (2015). Computing thermal bridge of vip in building

603 retrofits using designbuilder. *Energy Procedia*, 78, 400-405.

604 [37] Dachuan Shi, Yafeng Gao, Rui Guo, Ronnen Levinson, Zhi Sun, Baizhan Li. (2019). Life cycle
605 assessment of white roof and sedum-tray garden roof for office buildings in China. *Sustainable Cities and*
606 *Society*, 46 (2019) 101390.

607 [38] Crawley D., Lawrie L., Winkelmann F., Buhl W., Huang Y., Pedersen C., Strand K., Liesen R., Fisher
608 D., Witte M., Glazer J. (2001). EnergyPlus: Creating a new-generation building energy simulation
609 program, *Energy and Buildings*, (33) 319-331.

610 [39] Strand R.K., Modularization and simulation techniques for heat balance based energy and load calculation
611 programs: the experience of the ASHRAE loads toolkit and EnergyPlus. Seventh International IBPSA
612 Conference Rio de Janeiro, Brazil August 13-15,

613 [40] Zhuang, C. Q. (2016). *Research on the natural aging performance and energy-saving effect of thermal*
614 *reflection roof-- taking Xiamen dormitory building as an example*. Retrieved from Chongqing University.

615 [41] Ministry of Ecology and Environment of the People's Republic of China. (2016). *Technical Regulation*
616 *on Ambient Air Quality Index (on trial)*.

617 [42] Berdahl, P., Akbari, H., Levinson, R., Jacobs, J., Klink, F, Everman, R. (2012). Three-year weathering
618 tests on asphalt shingles: solar reflectance. *Solar Energy Materials and Solar Cells*, 99,277–281.

619 [43] Berdahl, P., Akbari, H., Levinson, R., Miller, W. A. (2008). Weathering of roofing materials—An
620 overview. *Constr. Build. Mater*, 22, 423–433, <http://dx.doi.org/10.1016/j.conbuildmat.2006.10.015>.

621 [44] Cao, X., Tang, B., Yuan, Y. (2016). Indoor and Outdoor Aging Behaviors of a Heat-Reflective Coating
622 for Pavement in the Chongqing Area. *Journal of Materials in Civil Engineering*, 28(1), 04015079.

623 [45] Levinson, R., Akbari, H. (2002). Effects of composition and exposure on the solar reflectance of Portland
624 cement concrete. *Cem. Concr. Res.*, 32, 1679–1698, [http://dx.doi.org/10.1016/S0008-8846\(02\)00835-9](http://dx.doi.org/10.1016/S0008-8846(02)00835-9).

625 [46] Mohamad Sleiman, Sharon Chen, Haley E.Gilbert, Thomas W.Kirchstetter, Paul Berdahl, Erica Bibian,
626 LauraS. Bruckman, Dominic Cremona, Roger H. French, Devin A. Gordon, Marco Emiliani, Justin
627 Kable, Liyan Mal, Milena Martarel lim, Riccardo Paolini, Matthew Prestia, John Renowden, Gian Marco
628 Revel, Olivier Rosseler, Ming Shiao, Giancarlo Terraneo, Tammy Yang, Lingtao Yu, Michele Zinzi,
629 Hashem Akbari, Ronnen Levinson, Hugo Destailats (2014). Soiling of building envelope surfaces and
630 its effect on solar reflectance-Part II: Development of an accelerated aging method for roofing materials.
631 *Solar Energy Materials & Solar Cells*, 122(3):271–281.

- 632 [47] Berdahl, P., Akbari, H., Rose, L. S. (2002). Aging of reflective roofs: soot deposition. *Applied Optics*, 41,
633 2355–2360.
- 634 [48] Lindberg, J. D., Douglass, R. E., & Garvey, D. M. (1993). Carbon and the optical properties of
635 atmospheric dust. *Applied Optics*, 32, 6077–6081.
- 636 [49] Sleiman, M., Ban-Weiss, G, Gilbert, H. E. (2011). Soiling of building envelope surfaces and its effect on
637 solar reflectance-Part I: Analysis of roofing product databases. *Solar Energy Materials & Solar Cells*,
638 95(12), 3385–3399.
- 639 [50] Cool Roof Rating Council (CCRC). *Rated products directory*. Available from
640 (<http://coolroofs.org/products/search.php>).
- 641 [51] Sproul, J., Man, P., Mandel, B., & Rosenfeld, A. (2014). Economic comparison of white, green, and black
642 flat roofs in the United States. *Energy & Buildings*, 71(3), 20–27.
- 643

644 **Figure captions**

645 Figure 1. Roofing products labeled with initial values of solar reflectance (ρ), thermal emittance (ϵ), lightness
646 color coordinate (L), red/green color coordinate (a), and yellow/blue color coordinate (b).

647 Figure 2. (a) Concrete tiles, (b) aluminum substrate specimens, (c) side view of the specimen holder; (d) top
648 view of the specimen holder.

649 Figure 3. Chinese climate zones, Chengdu and Xiamen cities location.

650 Figure 4. Natural outdoor-exposure of specimens (a) specimens location, and (b) exposure site.

651 Figure 5. (a) Axonometric rendering projection and (b) plan of the top floor of the representative dormitory
652 building simulated.

653 Figure 6. The solar reflectance of selected roofing products (aged - initial solar reflectance), (a)-(e) shows the
654 ten specimens exposed in Chengdu, while (f) shows the two specimens exposed in Xiamen.

655 Figure 7. Daily mean wind velocity, monthly mean air temperature, relative humidity and average precipitation
656 in Chengdu and Xiamen.

657 Figure 8. The monthly average Air Quality Index (AQI) in Chengdu and Xiamen (Dec 2014 or Jan 2015). AQI
658 presents the daily mean concentration of areal PM 2.5. Higher daily mean concentration indicates
659 higher the index level (i.e., I is excellent; II is good; III is light pollution; IV is moderate pollution)[41].
660 AQI data were provided by local weather stations with short distance to the exposure site.

661 Figure 9. Spectral reflectance within ranged 300nm–2500nm after every 3 months with 2%-sloped exposure
662 for coating(a) C6 (high lightness, cement-based) and (b) C7 (medium lightness, cement-based) in
663 Xiamen, (c) C3 (high lightness, cement-based),(d) C4 (medium lightness, cement-based), (e) C7
664 (high lightness, aluminum-based), and (f) C8 (medium lightness, aluminum-based) in Chengdu.

665 Figure 10. A feature of aged specimens in month 12s, (a) cracks, (b) blistering, and (c) mildew growth.

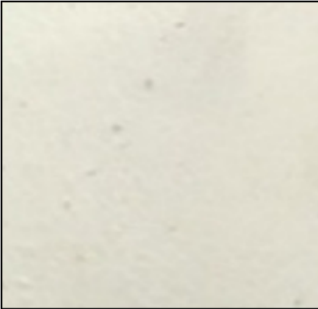


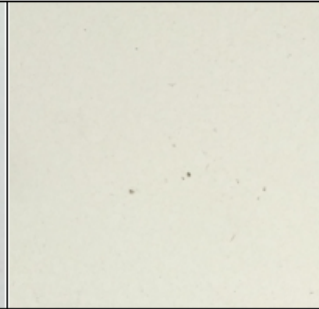
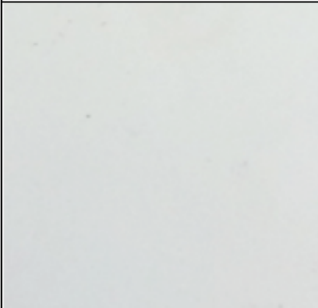
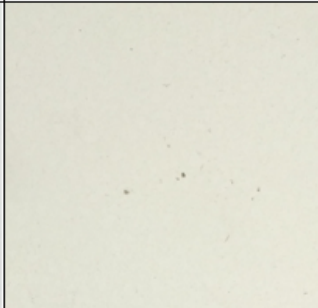
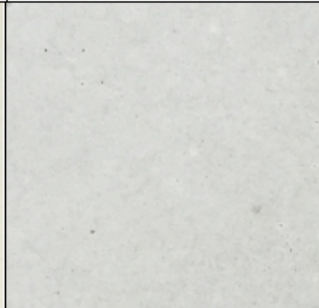
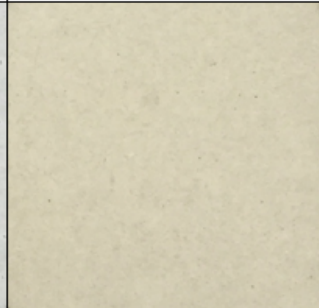
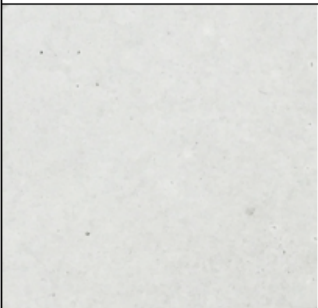


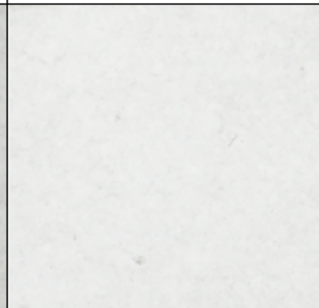
666 Figure 11. Annual heating and cooling loads and site energy consumption for dormitory building in Xiamen
667 with scenarios of the new or aged grey roof (albedo 0.20), aged cool roof (albedo 0.45), and new
668 cool roof (albedo 0.78).

669 Figure 12. Annual heating and cooling loads and site energy consumption for dormitory building in Chengdu
670 with scenarios of the grey roof (0.20), aged cool roof (0.56), and new cool roof (0.83).

671

672

673

			
WC-H-C ($\rho_i=0.88$; $\epsilon=0.85$) L: 96.34; a: -0.15; b: -0.55	BC-M-C ($\rho_i=0.56$; $\epsilon=0.85$) L: 86.43; a: 2.15; b: 18.55	CG-H-AL ($\rho_i=0.80$; $\epsilon=0.85$) L: 93.53; a: -1.20; b: -0.94	CG-M-AL ($\rho_i=0.77$; $\epsilon=0.85$) L: 91.39; a: -0.85; b: 9.77
			
CG-H-C ($\rho_i=0.82$; $\epsilon=0.86$) L: 94.64; a: -0.77; b: -0.40	CG-M-C ($\rho_i=0.77$; $\epsilon=0.87$) L: 91.65; a: -0.66; b: 10.21	DC-H-AL ($\rho_i=0.81$; $\epsilon=0.88$) L: 94.86; a: -0.74; b: 0.57	DC-M-AL ($\rho_i=0.75$; $\epsilon=0.89$) L: 89.56; a: 0.13; b: 16.27
			
DC-H-C ($\rho_i=0.83$; $\epsilon=0.90$) L: 94.31; a: -0.77; b: 1.28	DC-M-C ($\rho_i=0.75$; $\epsilon=0.93$) L: 89.81; a: 0.32; b: 16.68	SC-H-C ($\rho_i=0.88$; $\epsilon=0.89$) L: 96.90; a: -0.12; b: -0.23	SC-H-AL ($\rho_i=0.90$; $\epsilon=0.91$) L: 97.30; a: -0.17; b: -0.45

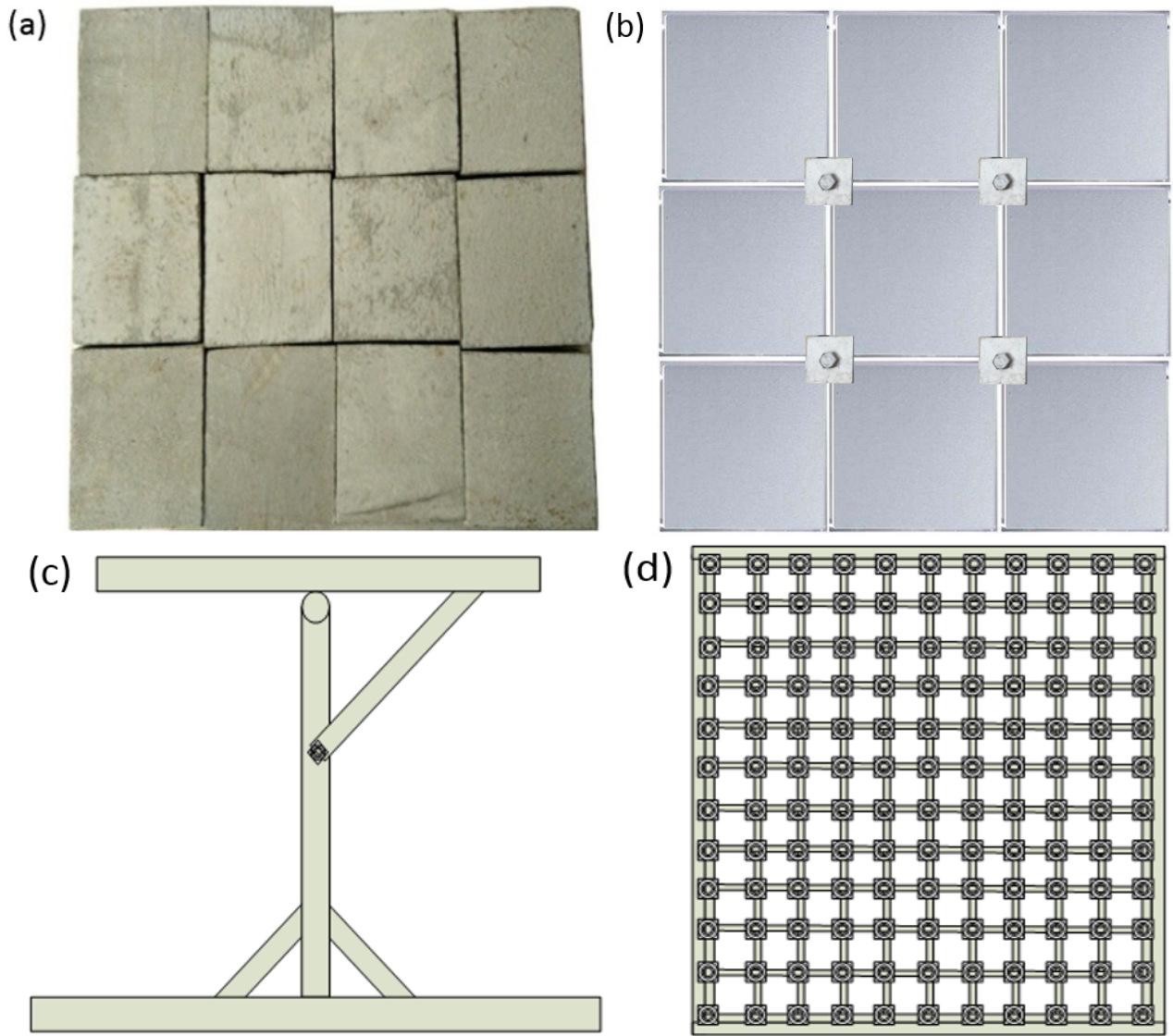
674

675

676

677

Figure 1. Roofing products labeled with initial values of solar reflectance (ρ), thermal emittance (ϵ), lightness color coordinate (L), red/green color coordinate (a), and yellow/blue color coordinate (b)



678

679

680

681

682

Figure 2. (a) Concrete tiles, (b) aluminum substrate specimens, (c) side view of the specimen holder; (d) top view of the specimen holder.

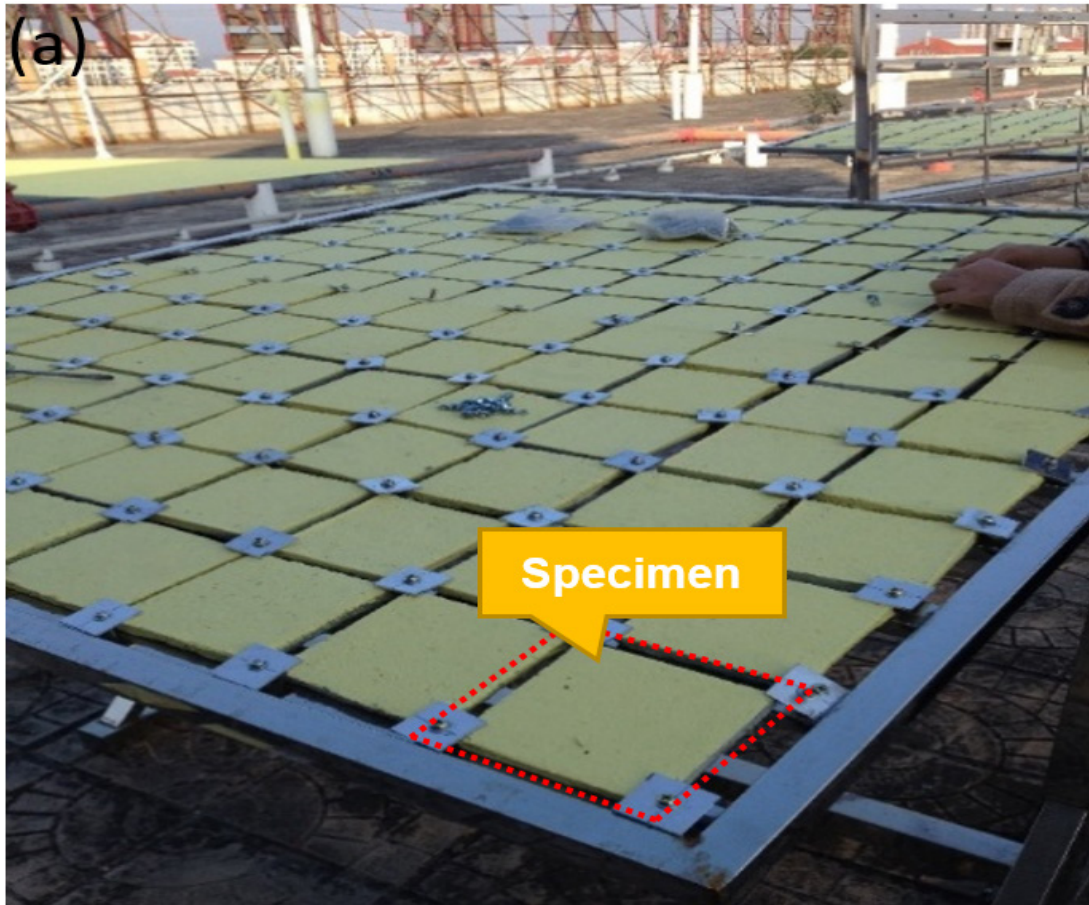


Figure 3. Chinese climate zones, Chengdu and Xiamen cities location.

683
684

685

686



687



688

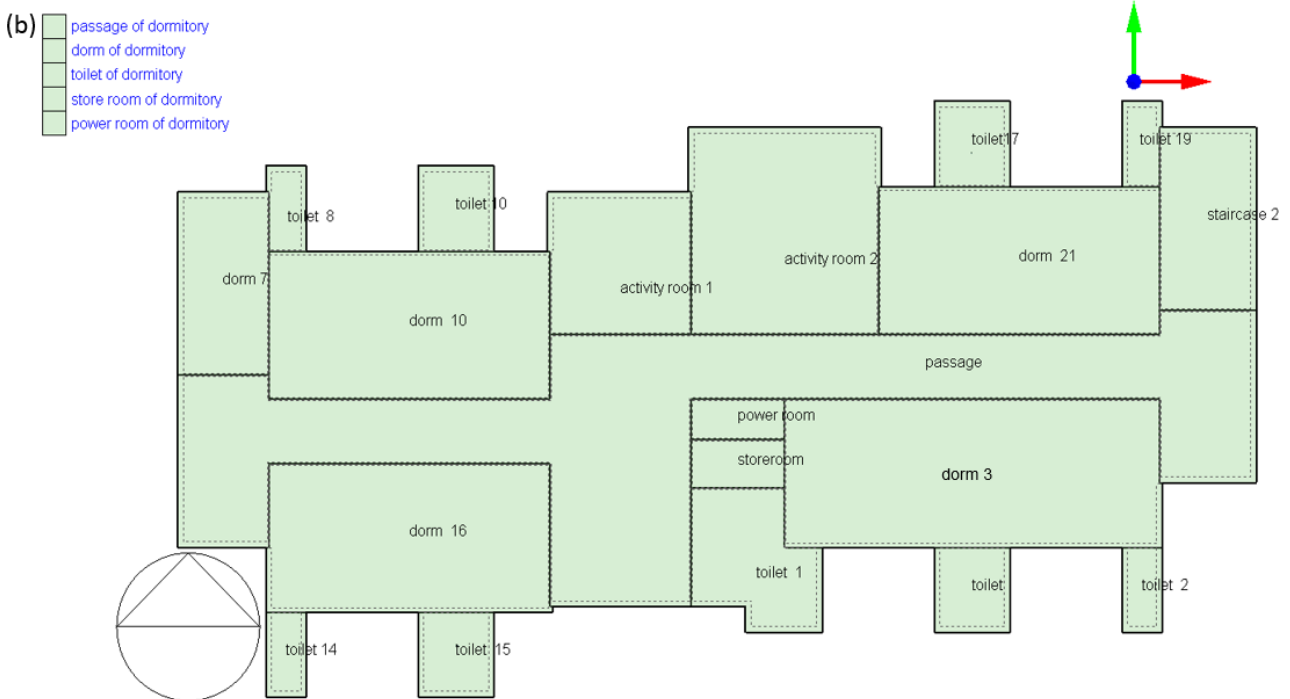
689

690

Figure 4. Natural outdoor-exposure of specimens (a) specimens location, and (b) exposure site.



691



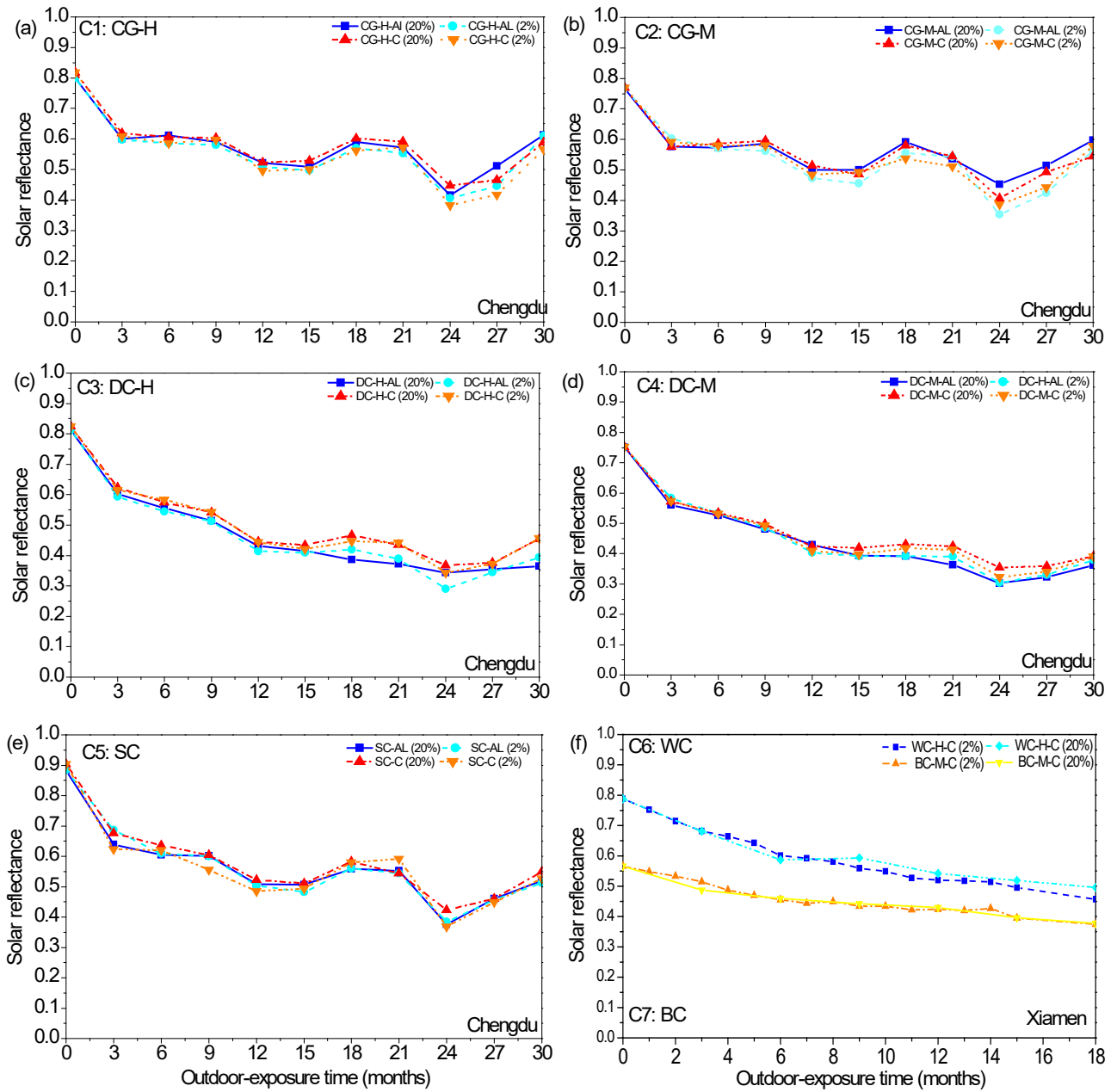
692

693

694

695

Figure 5. (a) Axonometric rendering projection and (b) plan of the top floor of the representative dormitory building simulated.



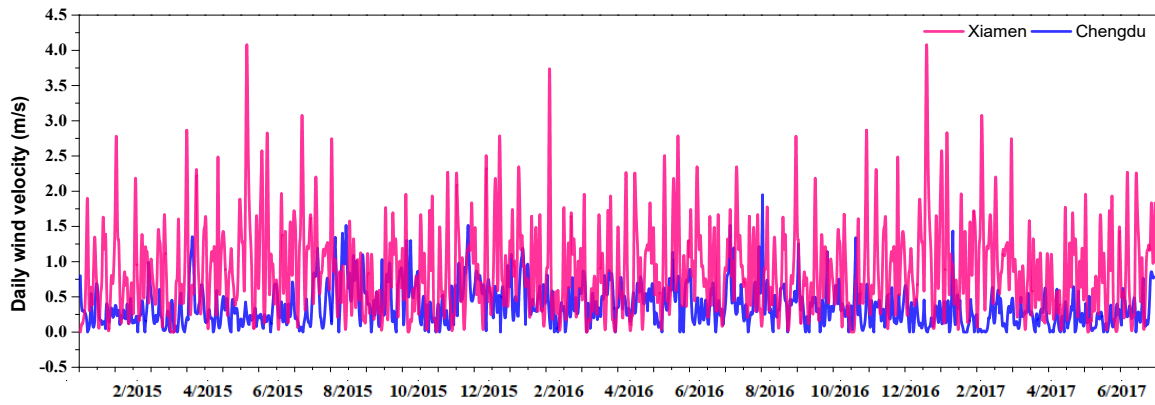
696

697

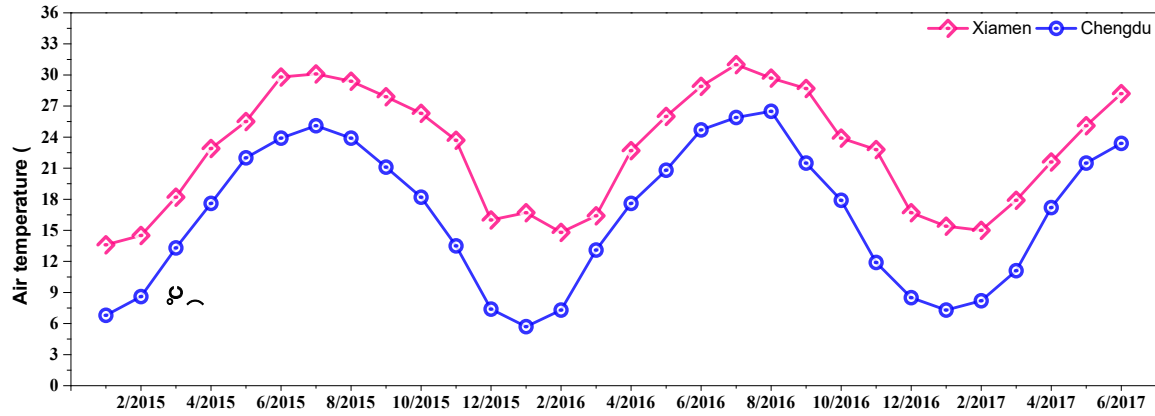
698

Figure 6. The solar reflectance of selected roofing products (aged - initial solar reflectance), (a)-(e) shows the ten specimens exposed in Chengdu, while (f) shows the two specimens exposed in Xiamen.

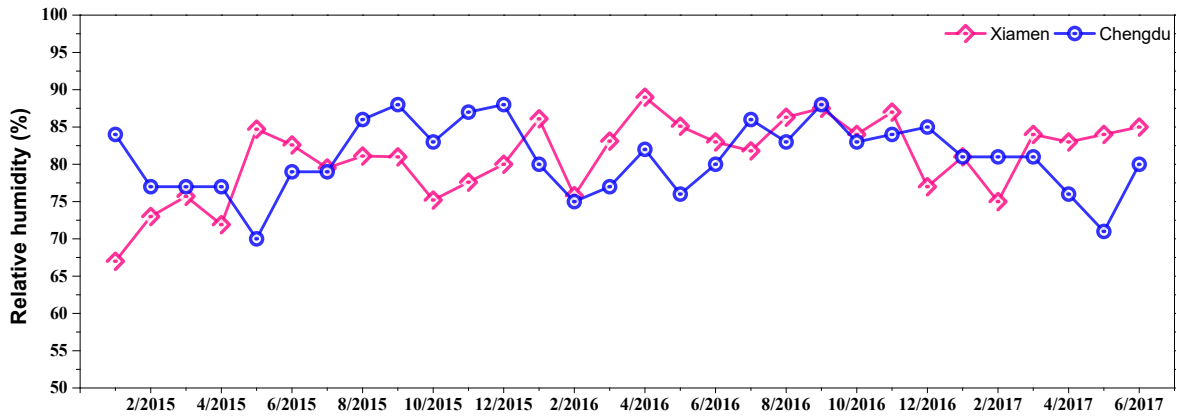
699



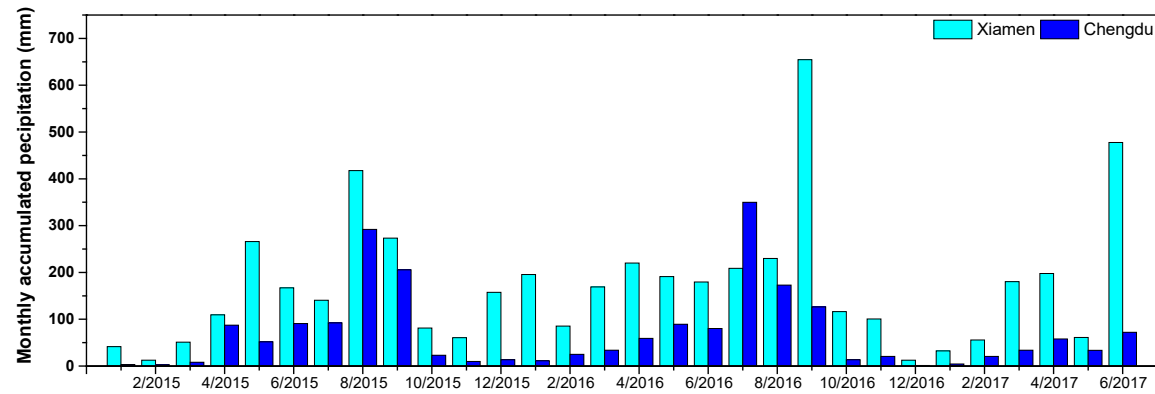
700



701



702



703

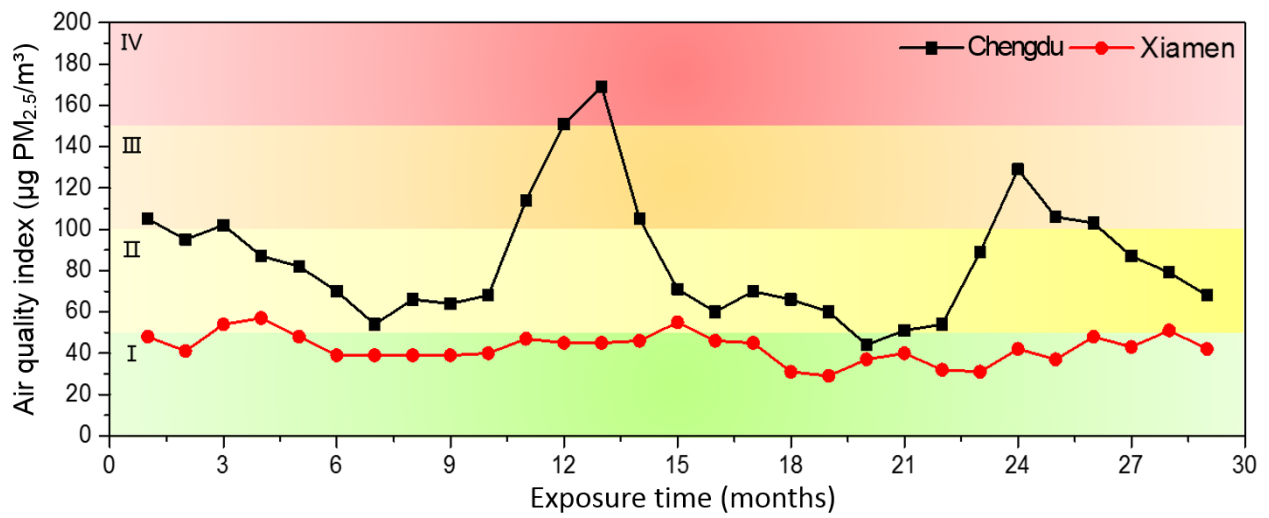
704

705

Figure 7. Daily mean wind velocity, monthly mean air temperature, relative humidity and average precipitation in Chengdu and Xiamen.

706

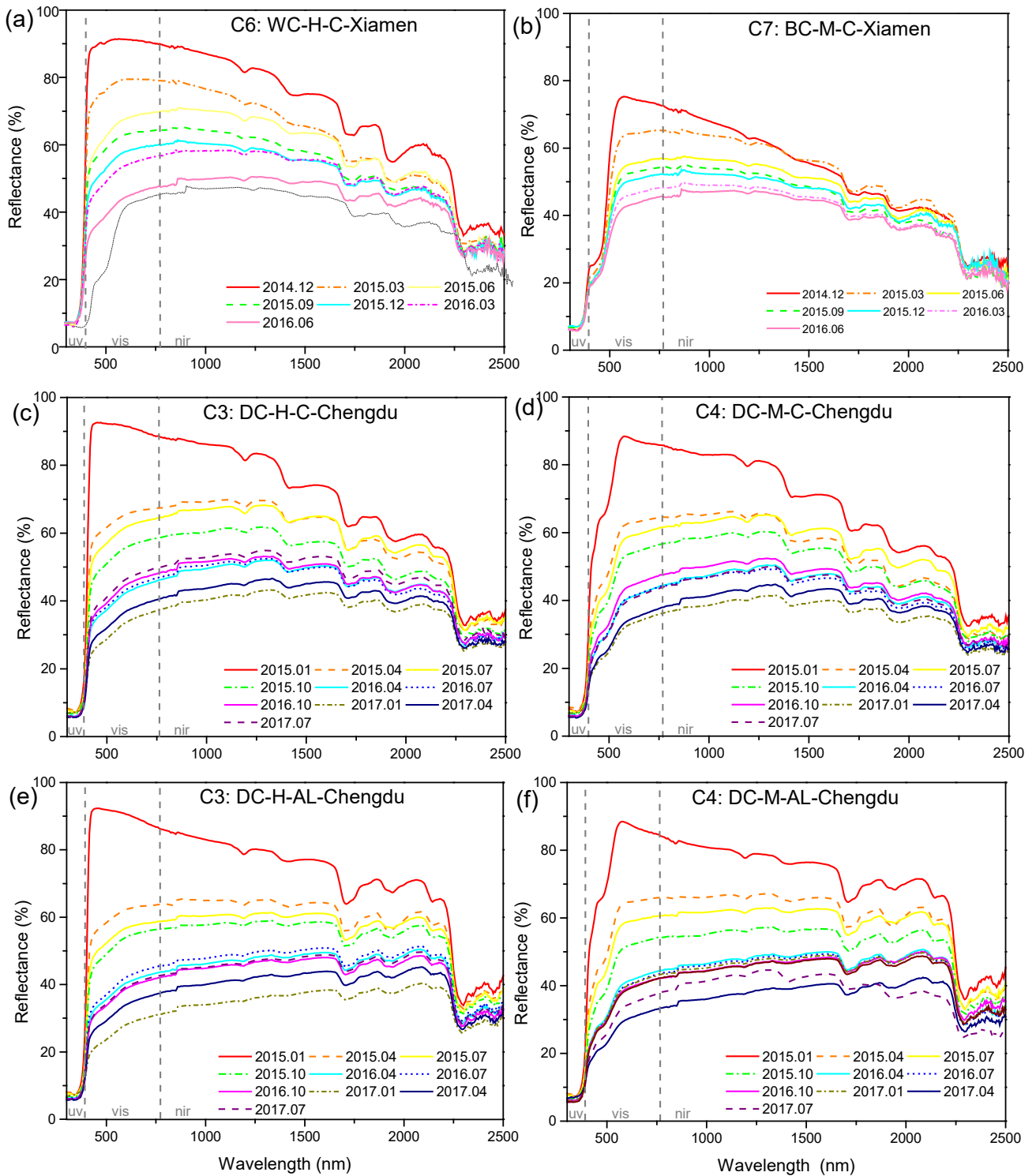
707



708

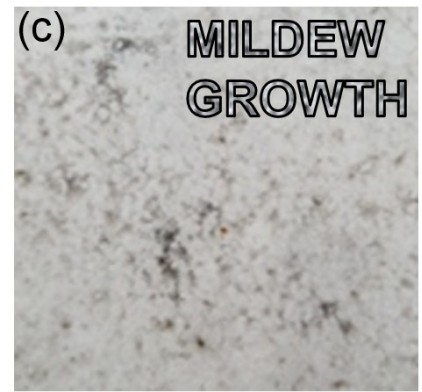
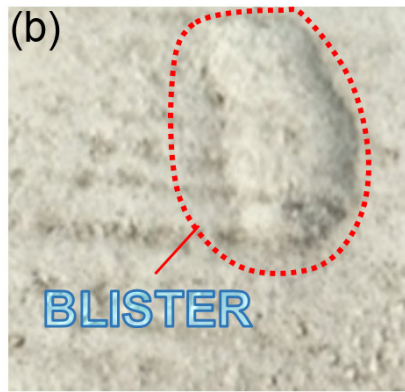
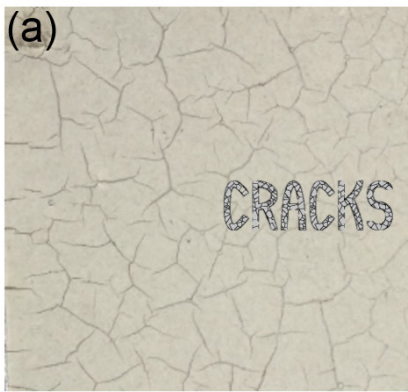
709 Figure 8. The monthly average Air Quality Index (AQI) in Chengdu and Xiamen (Dec 2014 or Jan 2015). AQI
 710 presents the daily mean concentration of areal PM 2.5. Higher daily mean concentration indicates higher the
 711 index level (i.e., I is excellent; II is good; III is light pollution; IV is moderate pollution)[41]. AQI data were
 712 provided by local weather stations with short distance to the exposure site.

713



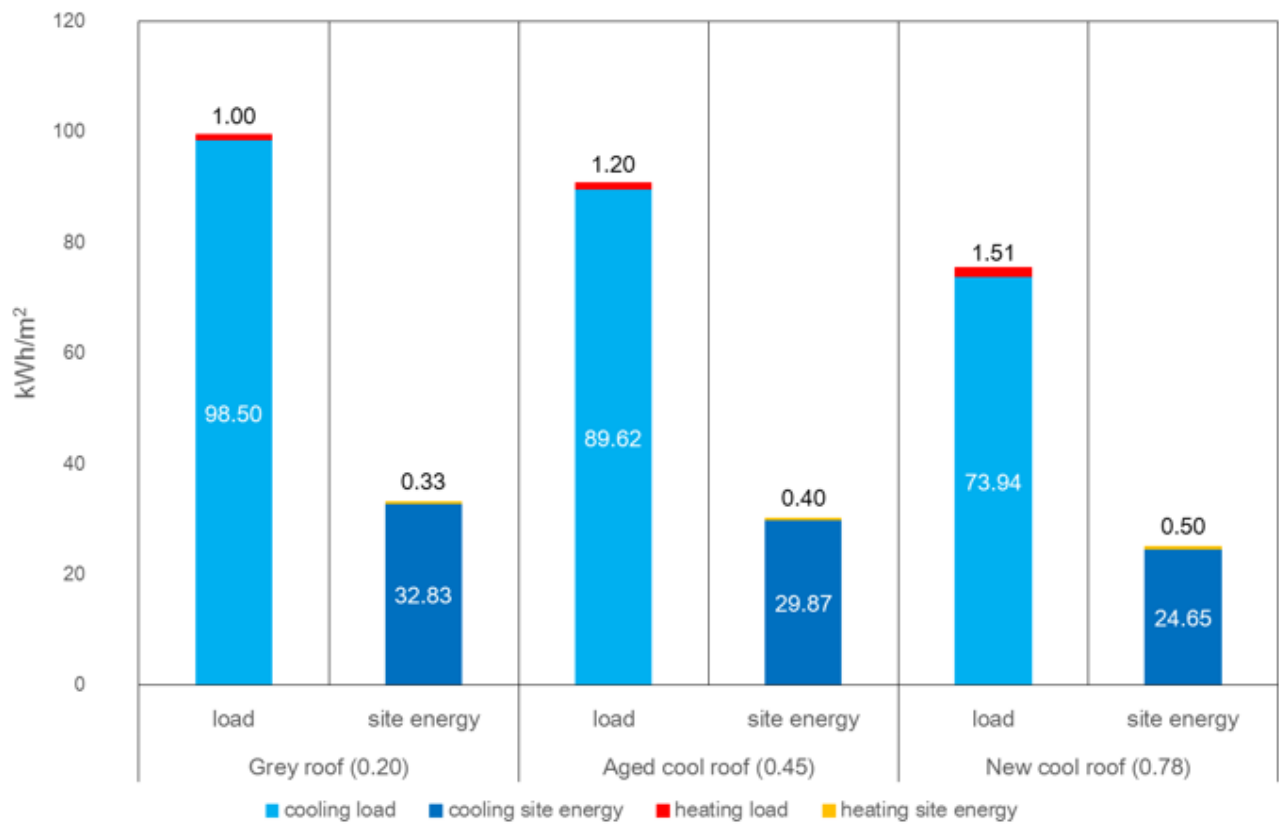
714
715
716
717
718
719

Figure 9. Spectral reflectance within ranged 300nm–2500nm after every 3 months with 2%-sloped exposure for coating(a) C6 (high lightness, cement-based) and (b) C7 (medium lightness, cement-based) in Xiamen, (c) C3 (high lightness, cement-based), (d) C4 (medium lightness, cement-based), (e) C7 (high lightness, aluminum-based), and (f) C8 (medium lightness, aluminum-based) in Chengdu.



720
721
722

Figure 10. A feature of aged specimens in month 12s, (a) cracks, (b) blistering, and (c) mildew growth.



723

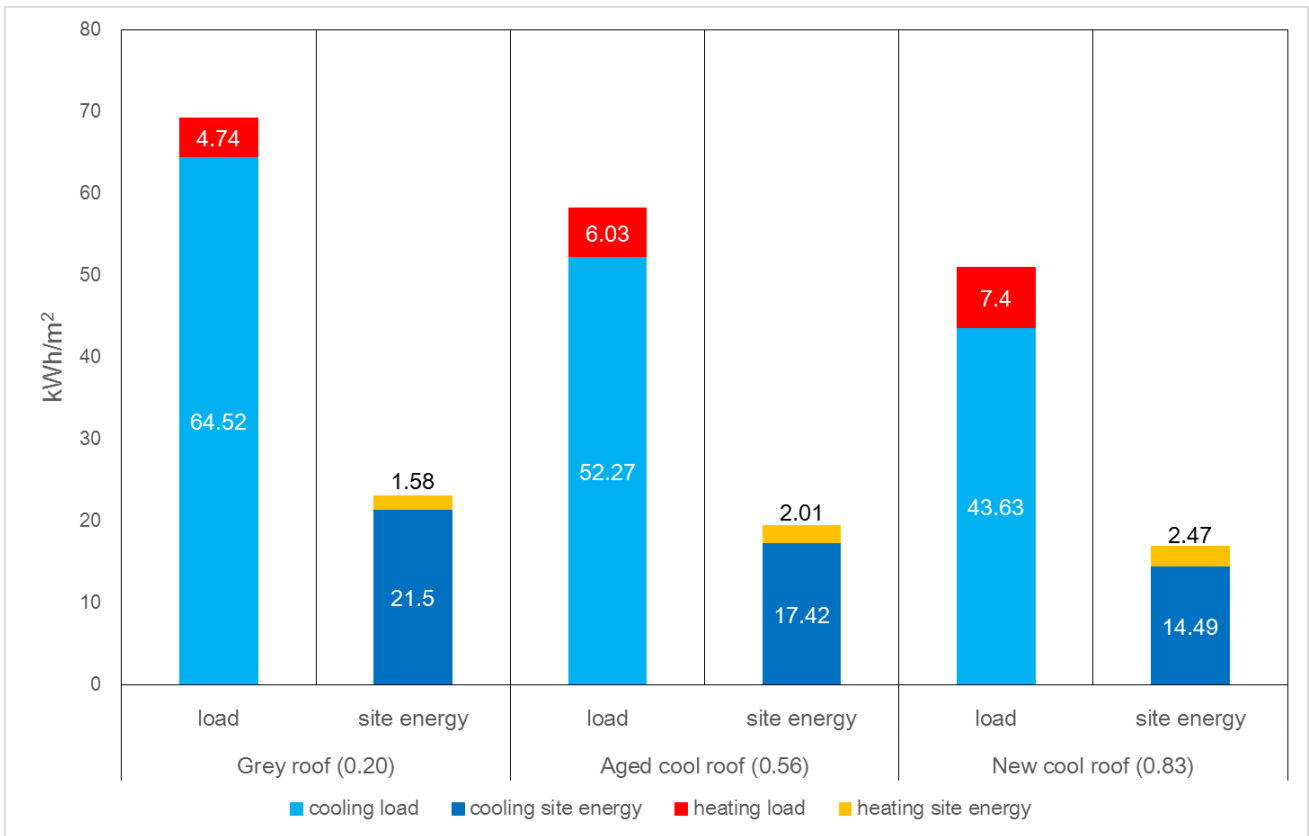
724

725

726

727

Figure 11. Annual heating and cooling loads and site energy consumption for dormitory building in Xiamen with scenarios of the new or aged grey roof (albedo 0.20), aged cool roof (albedo 0.45), and new cool roof (albedo 0.78).



728

729

730

731

Figure 12. Annual heating and cooling loads and site energy consumption for dormitory building in Chengdu with scenarios of the grey roof (0.20), aged cool roof (0.56), and new cool roof (0.83).

732 **Table captions**

733 Table 1. Selected high-reflectance roof coatings for the natural exposure trails in Xiamen and Chengdu.

734 Table 2. Characteristics of the top floor of the representative office building simulated.

735 Table 3. Roof and wall construction (listed outside to inside) of a representative office building in each city.

736 Table 4. High-reflectance roof standards in China.

737 Table 5. Solar reflectance and median values of selected roofing products after outdoor exposure in Xiamen
738 and Chengdu.

Table 1. Selected high-reflectance roof coatings for the natural exposure trails in Xiamen and Chengdu.

Experiment site	Code	Type ^a	Lightness	Substrate
Chengdu	C1	CG-H-AL/C	High	Aluminum/ Concrete Tile
	C2	CG-M-AL/C	Medium	Aluminum/ Concrete Tile
	C3	DC-H-AL/C	High	Aluminum/ Concrete Tile
	C4	DC-M-AL/C	Medium	Aluminum/ Concrete Tile
	C5	SC-H-AL/C	High	Aluminum/ Concrete Tile
Xiamen	C6	WC-H-C	High	Concrete Tile
	C7	BC-M-C	Medium	Concrete Tile

740
741
742

^aIn type X-Y-Z, X codes the manufacturer, Y codes the initial solar reflectance (H for high lightness or M for medium lightness), and Z codes the substrate (C for concrete tile or AL for aluminum).

Table 2. Characteristics of the top floor of the representative dormitory building simulated.

Layout	
Conditioned floor area, conditioned roof area (m ²)	626.3
Story height (m)	3.0
The ratio of window area to wall area	0.43 (south) 0.21 (north)
Building shape coefficient (surface-to-volume ratio) (m ⁻¹) ^a	0.26
Roof, wall, window thermal transmittance (W m ⁻² K ⁻¹)	0.9, 1.5, 4.0 ^a
Roof construction	See Table 3
Wall construction	See Table 3
Occupant density (person/m ²)	0.23 (room) ^b 0.1 (corridors) ^b
Occupancy hours (local standard time)	18:00–7:00 the next day (workdays) 00:00–24:00 (rest days and holidays)
Equipment load (W/m ²)	10 (bedroom), 3(toilet) ^b
Lighting load (W/m ²)	15 (room) ^b 5 (corridors) ^b
Cooling setpoint (°C)	26, with the setup to 28 ^b
Cooling schedule	18:00–7:00 the next day (workdays); 00:00–24:00 (rest days and holidays) ^c
Heating set point (°C)	16, with the setup to 12 ^b
Heating schedule	18:00–7:00 the next day (workdays) 00:00–24:00 (rest days and holidays)
Minimum fresh air via mechanical + natural ventilation (L/s-person)	8.33 ^b
Infiltration (ac/h)	1.0 ^a

744

^aSet based on JGJ 75-2012 Design Standard for Energy Efficiency of Residential Buildings in Hot Summer and Warm Winter Zone [37].

745

^bRecommended values for dormitory buildings in the DesignBuilder V5.3.

746

Table 3. Roof and wall construction (listed outside to inside) of a representative office building in each city [34].

City	Construction	Description	Thickness (mm)	Density (kg/m ³)	Specific heat per unit mass(kJ/kg·K)	Thermal conductivity W/(m·K)
Chengdu	Roof	Cement mortar	25	1800	1.051	0.930
		Polyurethane hard foam plastics	14	40	1.380	0.025
		Cement mortar	20	1800	1.051	0.930
		Lightweight aggregate concrete	80	1600	0.600	0.890
		Reinforced concrete	120	2500	1.220	0.590
	Wall	High elastic coatings	10	1200	1.000	0.930
		Polymer mortar	3	1800	1.050	0.930
		XPS extruded polystyrene board	11	28	2.100	0.030
		adhesive	20	1200	1.051	0.930
		Cement mortar	20	1800	1.051	0.930
		Clay porous brick	240	1400	1.051	0.580
		Mixed mortar	20	1700	1.051	0.870
		Xiamen	Roof	Fine stone concrete	40	2500
Extruded polystyrene board	30			30	1.386	0.030
Coil waterproof layer	2			600	1.465	0.175
Cement mortar	20			1800	1.050	0.930
Reinforced concrete	110			2500	0.920	1.740
Wall	Lime, cement, sand and mortar		25	1700	1.050	0.870
	Facing outside		5	1	0.001	1.000
	Concrete hollow block		190	1300	1.050	1.166
	Cement mortar		10	1800	1.050	0.930
	AC microcrystalline inorganic insulation mortar		25	350	1.050	0.090
Interior surface	5	1	0.001	1.000		

749

Table 4. High-reflectance roof standards in China.

Standard	ρ_i	Accelerated aging ^a albedo variation	ρ variation after soiling
Building Reflective Thermal- insulating Coatings (JG/T 235- 2014)	Low lightness	≥ 0.25	-
	Medium lightness	≥ 0.40	0.15
	High lightness	≥ 0.65	0.20

^aAccelerated aging, water-based (400h), solvent-type (500h).

750

751

752
753

Table 5. Solar reflectance and median values of selected roofing products after outdoor exposure in Xiamen and Chengdu.

	Albedos of selected coatings		
	Initial	Month 30	Median values at month 30
Xiamen	0.57-0.78	0.37-0.50	0.45
Chengdu	0.75-0.90	0.36-0.62	0.56

754